CrossMark

ORIGINAL RESEARCH

Synthesis and characterization of $Ln_2O_2SO_4$ (Ln = Gd, Ho, Dy and Lu) nanoparticles obtained by coprecipitation method and study of their reduction reaction under H_2 flow

Sèmiyou. A. Osseni[1,2] · Yu. G. Denisenko[2] · Jacques. K. Fatombi[3] ·
Elena. I. Sal'nikova[2,4] · Oleeg. V. Andreev[2]

Abstract We have proposed an optimized homogeneous precipitation method for the synthesis of spherical and well-dispersed pure $Ln_2O_2SO_4$ (Ln = Gd, Ho, Dy and Lu) nanoparticles (NPs) using synthesized lanthanide sulfates and urea as starting materials. $Ln_2O_2SO_4$ NPs can be easily transformed to Ln_2O_2S by reduction under H_2 flow at 650 °C for Gd, Dy and Ho whereas the reduction with Lu gave only Lu_2O_3. Particle size was between 500 nm and 3.5 μm. This reduction method allows to obtain Ln_2O_2S without using H_2S which is highly toxic and uncomfortable gas. $Ln_2O_2SO_4/Ln_2O_2S$ synthetized can be used for release and oxygen storage or doped with luminescent centers for multimodal medical imaging applications.

✉ Sèmiyou. A. Osseni
    osema28@yahoo.fr

1   Department of Chemistry, Faculty of Sciences and Technology of Natitingou, UNSTIM, Abomey, Benin

2   Institute of Chemistry, Tyumen State University, Perekopskaya Str. 15a, Tyumen 625003, Russia

3   Laboratory of Water Chemistry and Environment-ENS, UNSTIM, Abomey, Benin

4   Northern Trans-Ural State Agricultural University, Tyumen, Russia

Springer

Graphical abstract
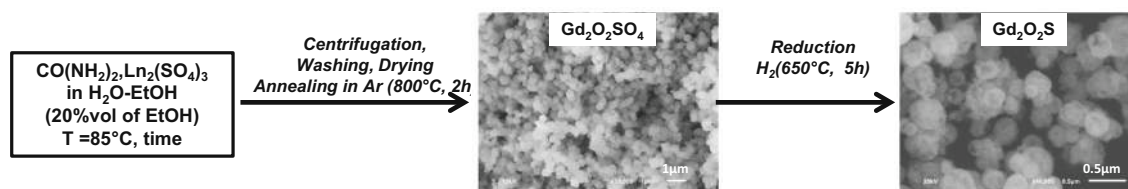
Introduction

During this last decade, lanthanide oxysulfate and oxysulfide compounds (Ln = Gd, Ho, Dy and Lu) have been widely used due to their applications in phosphorescent material design, X-ray-computerized tomography, oxygen storage, and radiation detection [1–3]. The other remarkable features of lanthanide oxysulfide/oxysulfate are their large accurate sensing capability over a wide range of temperatures, as well as their ability to withstand a harsh environment [4]. Moreover, the crystal structure of $Ln_2O_2SO_4$ is usually the alternative stacking of a $[Ln_2O_2]^{2+}$ layer and a layer of sulfate $[SO_4]^{2-}$ and that of Ln_2O_2S is the alternative stacking of a $[Ln_2O_2]^{2+}$ layer and a layer of sulfide (S^{2-}) [5]. Thus, $Ln_2O_2SO_4$ is an intermediate phase for the synthesis of lanthanide oxysulfide Ln_2O_2S and is usually used as a precursor for the synthesis of Ln_2O_2S in reduction atmosphere.

The $Ln_2O_2SO_4$ materials for oxygen storage and release reported so far have been prepared by several methods, such as calcination of $Ln(SO_4)_3 \cdot nH_2O$ [6–8], solid-state reaction method using lanthanide oxide and diammonium hydrogen sulfate as the starting materials [9, 10], utilization of precursors of layered Ln-dodecyl sulfate mesophases' [11], Ln-precipitation [12, 13], thermal decomposition of nanodroplets formed by Ln-acetylacetonates ($Ln(acac)_3$) [14] and hydrothermal decomposition of hydroxyl sulfates of $Ln_2(OH)_4SO_4$ (Ln = Eu-Lu and Y) [15] .

All of these methods result to bulk materials with an irregular morphology. The synthesis of NPs intended for applications in imaging and medical therapy imposes the control of many physicochemical characteristics such as the crystal structure and the morphology of the particles. The soft chemistry processes for preserving texture, morphology and structure are, therefore, well adapted for the development of these NPs [16]. The homogeneity of the particles obtained, the control of the various steps of germination and growth of the crystallites originating from the liquid are the main advantages of these synthesis processes. Homogeneous precipitation synthesis is one of the most promising techniques because of its advantages such as the relatively simple synthetic route, low cost, ease of mass production.

Lian et al. [17]. have synthesized $(Gd_{1-x}Eu_x)_2O_2SO_4$ sub-microphosphors by homogeneous precipitation method from commercially available Gd_2O_3, Eu_2O_3, H_2SO_4 and $(NH_2)_2CO$ (urea) starting materials. After precipitation reaction, the precursor which is mostly composed of gadolinium hydroxyl, carbonate and sulfate groups with some crystal water; can be transformed into pure $Gd_2O_2SO_4$ phase after heating at 900 °C for 2 h in air. They reported that it is only when the molar ratio of urea to $Gd_2(SO_4)_3$ is equal to 5, there is formation of pure $Gd_2O_2SO_4$ phase. The particles were quasi-spherical with a mean size of about 500 nm. The same authors have also reported [18] the photoluminescence of $(Gd_{1-x}Dy_x)_2O_2SO_4$ using the same method. In that work, they use molar ratio of urea to $Gd_2(SO_4)_3$ equal to 400, to form pure $Gd_2O_2SO_4$ phase. Thus, there is no clearly in literature the optimal conditions about molar ratio of urea to $Ln_2(SO_4)_3$ that can be used to synthesize $Ln_2O_2SO_4$ NPs by homogeneous precipitation method.

This paper suggested an optimized homogeneous precipitation method to prepare spherical and well-dispersed pure $Ln_2O_2SO_4$ and Ln_2O_2S (Ln = Gd, Ho, Dy and Lu) NPs using synthesized lanthanide (Ln = Gd, Dy, Ho and Lu) sulfates and urea as starting materials. Then, we studied the reduction reaction of $Ln_2O_2SO_4$ under H_2 to form Ln_2O_2S to avoid the use of dangerous sulfur-based gases.

Experimental section

Materials and method

Gadolinium, dysprosium, holmium and lutetium sulfate were synthesized at our laboratory. Urea (99%) was purchased from Reaktiv OAO (Saint-Petersburg, Russia).

Precursors were prepared by coprecipitation method as previously described [1, 2, 19] with some modifications using lanthanide (Ln = Gd, Dy, Ho and Lu) sulfates in deionized water and ethanol, using a protocol based on the decomposition of urea at temperatures around 85 °C. The optimum concentration employed in this study was

$[Ln^{3+}] = 5.6 \times 10^{-3}$ M. The concentration of urea was varied (0.125, 0.25 and 0.5 M). So molar ratio of urea to Ln^{3+} was equal to $r = 22.3$, 44.6 and 89.3. Solvent employed was deionized water–ethanol with 20 vol% of ethanol. Gd, Dy, Ho and Lu sulfates and urea were dissolved in the solvent, and the solution was placed in a round-bottom flask at reflux for aging at 85 °C in an oil bath, during 120 min for a total volume of 2L under vigorous stirring. The suspension was then centrifuged for 10 min at 6000 rpm. The supernatant of the solution is removed and the solid phase is suspended in deionized water for washing. The solid is dried in an oven at 80 °C overnight.

The precursors were heated at 800 °C during 2 h (5 °C/min) in argon to form $Ln_2O_2SO_4$ (Ln = Gd, Ho, Dy and Lu) NPs.

In our previous work [1, 20, 21], lanthanide oxysulfides were prepared by sulfuration using Ar-H_2S gas or H_2-S mixture. Unfortunately, H_2S is highly toxic and uncomfortable to work with. Therefore, for preparation of oxysulfides we adopted reduction of lanthanide oxysulfates in H_2 flow. Ln_2O_2S (Ln = Gd, Ho, Dy and Lu) NPs were synthesized by heating $Ln_2O_2SO_4$ (Ln = Gd, Ho, Dy and Lu) NPs at 650 °C during 5 h in H_2 to form Ln_2O_2S.

Characterization techniques

X-ray diffractometry (XRD) measurements were performed on a DRON3 X-ray diffractometer using Co-Kα radiation (1.79021 Å). The data were collected with 2θ value from 5° to 80°.

The determination of the different chemical bonds was made by infrared spectroscopy, using a PerkinElmer 100 Series spectrometer. The pellets were prepared by mixing the powders with potassium bromide (1/100 by weight).

Thermal analysis, i.e., thermogravimetry (TG) and differential thermal analysis (DTA), was performed using a Netzsch STA 449 F 3 Jupiter system. DTA and TG with 10 °C/min heating rate in the argon were done on the sample of 50 mg at the same time.

The particle morphology of the synthesized products was observed by a JEOL JSM-6510LV scanning electron microscope (SEM).

Results and discussion

XRD and SEM characterization of NPs

The XRD pattern of precursor (not shown here) did not reveal diffraction peaks. This observation is specific to amorphous or disordered compounds. Figure 1 shows the diffractograms of the precursors with various molar ratio of
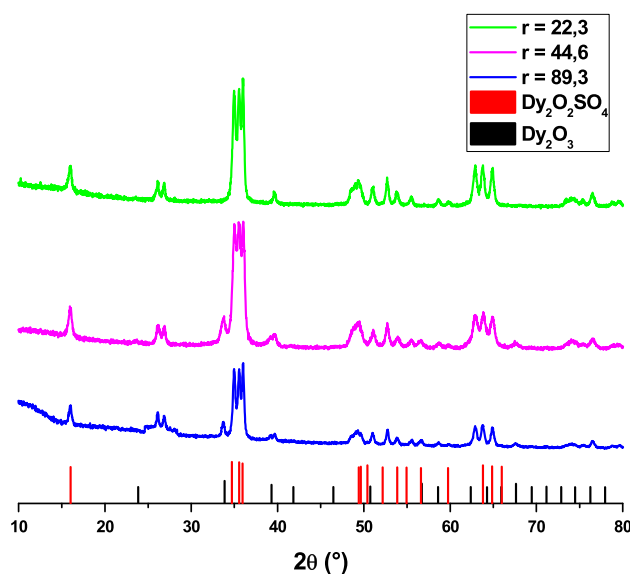

Fig. 1 XRD patterns of product obtained from Dy precursor after annealing at 800 °C during 2 h (5 °C/min) in argon

urea to Ln^{3+} after annealing in argon at 800 °C. When the molar ratio r is equal to 89.3 [(urea) = 0.5 M], the final products obtained are mainly composed of $Ln_2O_2SO_4$ and a small amount of Ln_2O_3. With decreasing of r values to 22.3 [(urea) = 0.125 M], the disappearance of Ln_2O_3 diffraction peaks can be observed, indicating that more OH^- or CO_3^{2-} anions are substituted by SO_4^{2-} anions as a result of excess of $Ln_2(SO_4)_3$ dosage during homogeneous precipitation. Thus, the concentration of urea ($r = 22.3$) is chosen as the best condition in the rest of our work.

The XRD patterns (Fig. 2) of the final products of all lanthanides (Ln = Gd, Ho, Dy and Lu) exhibit well-developed peaks, characteristic of lanthanide oxysulfate phases without precipitation of impurities.

The lattice parameters were calculated and could be indexed to the orthorhombic phase of $Ln_2O_2SO_4$ matched

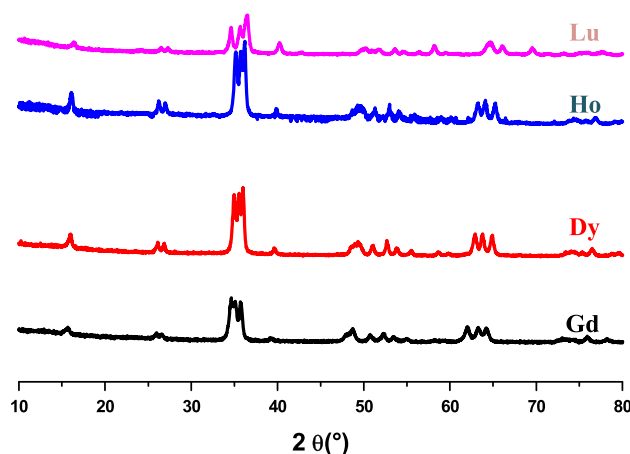**Fig. 2** XRD patterns of $Ln_2O_2SO_4$ NPs obtained after annealing of precursor in Ar at 800 °C (2 h)

with the standard of the literature values [22] and presented in Table 1.

Figure 3 shows XRD patterns of reduction of $Ln_2O_2SO_4$ (Ln = Gd, Dy and Ho) particles in H_2 at 650 °C during 5 h. The patterns show well-developed peaks, characteristic of hexagonal lanthanide oxysulfide phases for Gd, Dy and Ho. All peaks are indexed according the ICDD data in the hexagonal phase, of Gd_2O_2S(File card No 020-1422), Dy_2O_2S(File card No 026-0592) and of Ho_2O_2S(File card No 025-1143), respectively, for Gd, Dy and Ho. No additional peak from impurities can be detected.

For Lu, reduction in H_2 gave only lutetium oxide: Lu_2O_3 (XRD patterns not shown here) even though the reduction temperature was changed to 650, 690, and 800 °C.

Transformation of $Ln_2O_2SO_4$ to Ln_2O_2S is commonly classified as a redox reaction and can be described by the equation:

$$Ln_2O_2SO_4 + 4H_2 \rightarrow Ln_2O_2S + 4H_2O \quad (Ln = Gd, \ Dy \ and \ Ho)$$

$$(1)$$
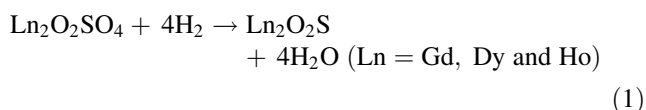
For Lu, the presence of only lutetium oxide: Lu_2O_3 can be described by the equation:

$$Lu_2O_2SO_4 + 4H_2 \rightarrow Lu_2O_3 + SO_2 + 4H_2O \quad (2)$$
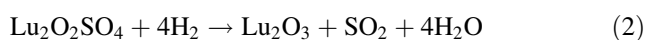
These results are consistent with those reported by Andreev et al. [20, 21] on the transformation of $Ln_2O_2SO_4$ bulk materials obtained by solid-state reaction to Ln_2O_2S under H_2 flow.

SEM images corresponding to each $Ln_2O_2SO_4$ before and after reduction are showed in Fig. 4. Before reduction, NPs are spherical and monodispersed in size with a mean diameter of 500 nm, 3.5 μm, 1.7 μm and 1.2 μm respectively for Gd, Dy, Ho and Lu. After reduction, the morphology of particles is conserved with a reduction in size with a mean diameter of 310 nm, 2.8 μm, 830 nm and 1 μm respectively for Gd, Dy, Ho and Lu. The difference in morphology observed could be explained by a difference in the reactivity of these lanthanides during the precipitation reaction and the effect of the famous "contraction of the lanthanides". In fact, the particle size is significantly

Fig. 3 XRD patterns of: Ln_2O_2S particles obtained after reduction in H_2 at 650 °C during 5 h (5 °C/min)
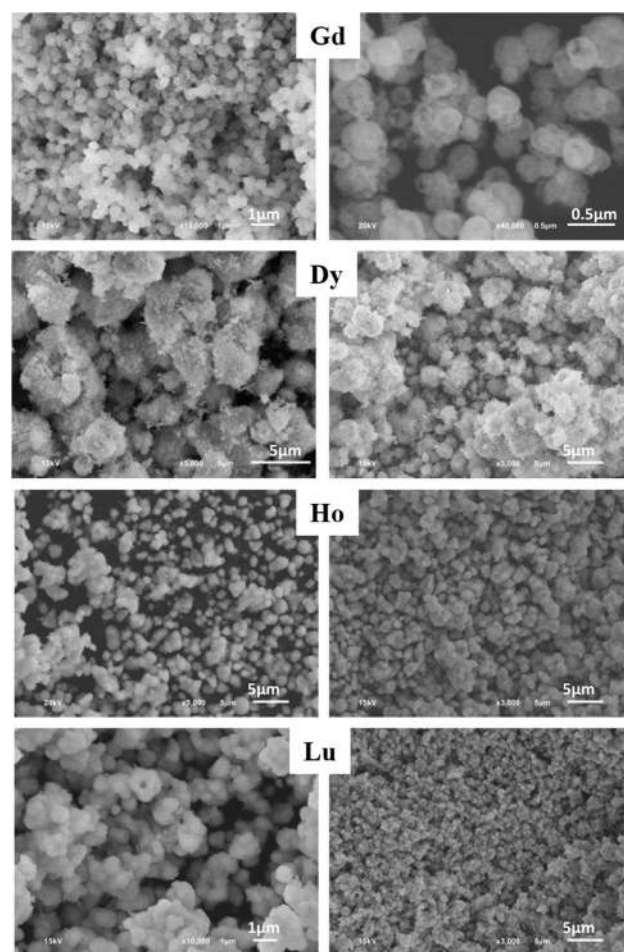
Fig. 4 SEM images of $Ln_2O_2SO_4$: before (left) and after (right) reduction in H_2 at 650 °C (5 h)

Table 1 Lattice parameters of $Ln_2O_2SO_4$ (Ln = Gd, Ho, Dy and Lu)

Samples	Standardized parameters			Calculated parameters		
	a (Å)	b (Å)	c (Å)	a (Å)	b (Å)	c (Å)
$Gd_2O_2SO_4$	4.062	4.188	12.96	4.0638	4.1791	12.9840
$Dy_2O_2SO_4$	4.152	4.026	12.76	4.1497	3.9741	12.7508
$Ho_2O_2SO_4$	4.142	4.012	12.73	4.1451	3.9580	12.7213
$Lu_2O_2SO_4$	4.108	3.961	12.42	4.1065	3.9571	12.4207

affected by a decrease in the effective ionic radius of the lanthanide ions. Reducing the radius with a simultaneous increase in the nuclear charge leads to an increase in the tendency of the particles to agglomerate. In our SEM pictures observation, two types of particles were identified. The particles sizes differ from nanoscale and monodisperse (Gd) to microscale (Ho, Dy, Lu). This division is not accidental. The synthesized compounds of gadolinium enter into the region of crystal-chemical instability and in their properties are similar to compounds of light rare-earth elements. While the elements from terbium to lutetium are heavy. Within the series of heavy rare earth elements, two families are distinguished: similar terbium (Tb-Tm, Y) and similar ytterbium (Yb-Lu). Thus, the differences in particle morphology are caused by the fact that compounds are formed by rare earth elements being representatives of different families.

FT-IR spectroscopy characterization of NPs

Figure 5 showed FT-IR analysis spectra of precursor and its annealed product for each lanthanide.

The FT-IR spectrum of the precursor for each lanthanide (Fig. 5a) shows bands attributed to the absorption peaks of physically absorbed water, crystal water, hydroxyl groups [23] (near 3500 and 1610 cm^{-1}), the CO_3^{2-} (near 1450 cm^{-1}) and the SO_4^{2-} anions (near 1125 and 680 cm^{-1}), which shows that the precursor is consisted of lanthanide, hydroxyl, carbonate and sulfate groups with some crystal water. After calcination under argon at 800 °C (Fig. 5b), spectrum showed that the peak centered at 3500 cm^{-1} becomes weak, indicating that the removal of crystal water from the precursor. The SO_4^{2-} absorption bands (near 1125 and 625 cm^{-1}) split into some narrow

sharp peaks, the absorption bands become weaker, and a new small absorption peak centered about 500 cm^{-1} appears, which corresponds to the characteristic vibration peaks of Ln–O bond in the prepared product. These observations are very similar to the ones already discussed in the previous work [1, 17, 18]. We, thus, conclude that the formulation of the NPs elaborated in a water–EtOH (80–20 vol%) mixture is $Ln_2(OH)_2CO_3SO_4 \cdot xH_2O$ (Ln = Gd, Dy, Ho and Lu), the lanthanide hydroxycarbonate sulfate. This precursor has been well transformed into $Ln_2O_2SO_4$ (Ln = Gd, Ho, Dy and Lu) after annealing in argon at 800 °C.

DTA-TG characterization of NPs

The TG/DTA curves (Fig. 6) show the thermal decomposition under argon atmosphere of precursor Dy precursor and offer interesting result to complete the determination of its formula. The TG curve presents a continuous weight loss between 80 and 900 °C with an overall weight loss of approximately 17 wt%. This total weight loss mainly consists of the following steps in the whole temperature range. The weight loss in the temperature range from room temperature to $\approx$ 300 °C is about 7.5% by mass and represents the progressive removal of physically absorbed water from the precursor. This mass loss corresponds to a weak endothermic peak at around 160 °C in DTA curve. The weight loss between 300 and 500 °C is about 4.1% by mass, which is associated with the complete dehydroxylation of the precursor with the progressive decomposition of CO_3^{2-} anions and emission CO_2. This weight loss corresponds to an endothermic peak at 450 °C in the DTA curve. The weight loss in the temperature range from 500 to 693 °C is about 5.4% by mass, which is attributed with

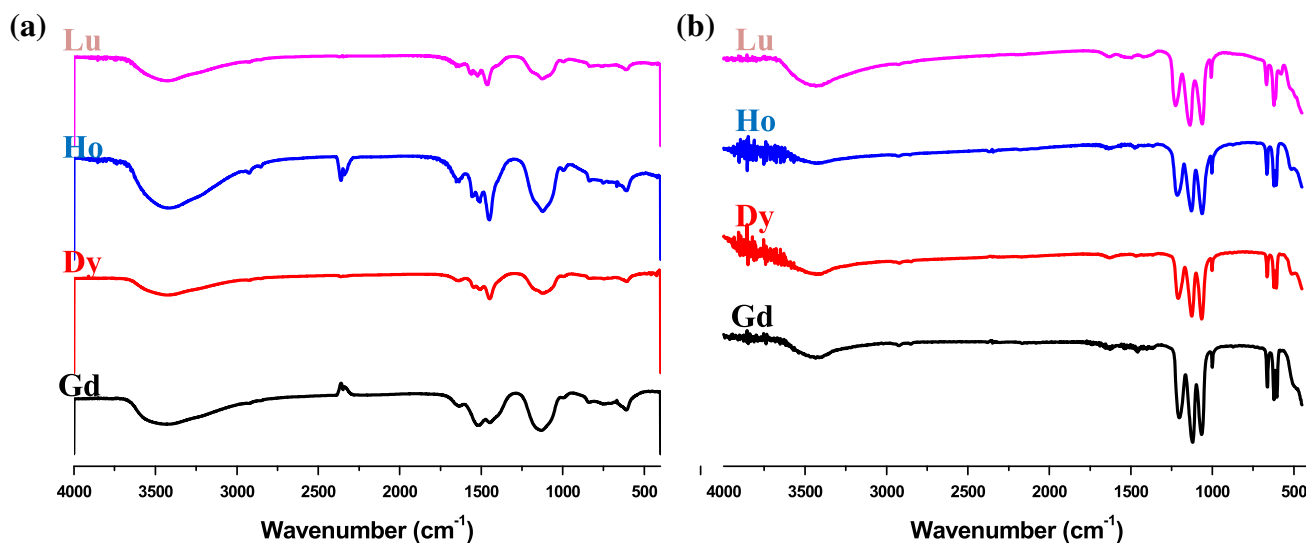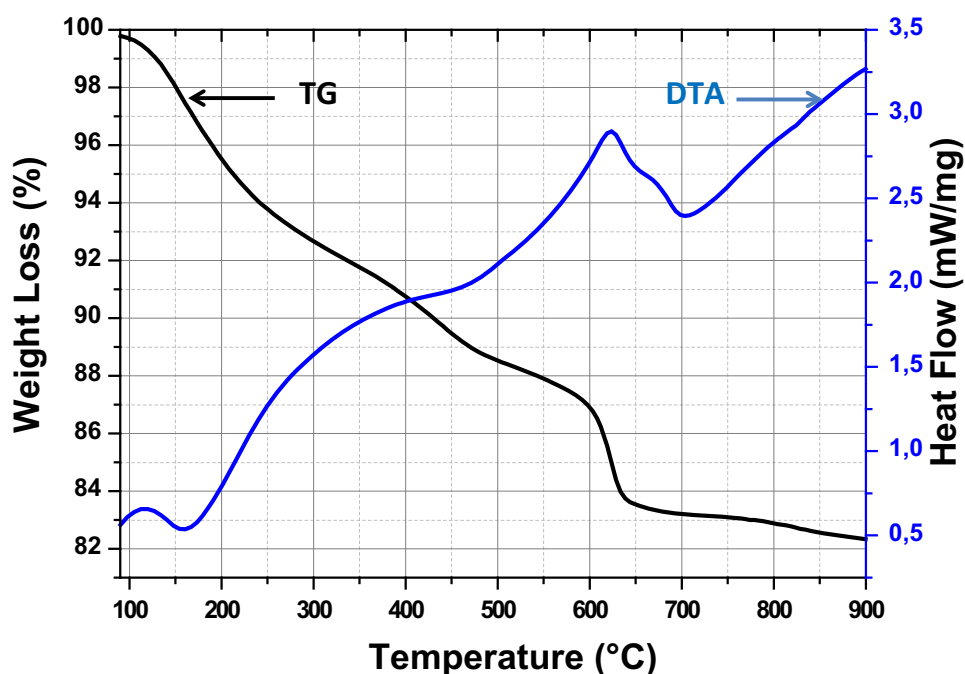**Fig. 5** FT-IR spectra of: **a** precursor and **b** $Ln_2O_2SO_4$ particles

Fig. 6 TG-DTA curves of Dy precursor in argon

the full decomposition of CO_3^{2-} anions and release CO_2 of the precursor. Moreover, as shown in Fig. 6, small variations in mass are observed at temperatures higher than 750 °C on the TG curve. This is why we used 800 °C as the optimal heat treatment temperature for the synthesis of $Ln_2O_2SO_4$ particles. The same thermal decomposition (Curves not shown here) was observed for Gd, Ho and Lu precursor. Thus, the formula of precursor is $Ln_2(OH)_2$-$CO_3SO_4 \cdot xH_2O$ (Ln = Gd, Dy, Ho and Lu). These results are in a good agreement with those reported previously [17, 18] and with those obtained by FTIR analyses and XRD patterns.

Conclusions

We have proposed an optimized homogeneous precipitation method to synthesize spherical and well-dispersed pure $Ln_2O_2SO_4$ (Ln = Gd, Ho, Dy and Lu) NPs with size between 500 nm and 3.5 μm. If $Ln_2O_2SO_4$ NPs can be easily transformed to Ln_2O_2S by reduction under H_2 flow at 650 °C for Gd, Dy and Ho, Lu gave only Lu_2O_3 under H_2 flow even though the reduction temperature was changed to 650, 690, and 800 °C. This reduction method allows to obtain Ln_2O_2S without using H_2S which is highly toxic and uncomfortable gas. $Ln_2O_2SO_4/Ln_2O_2S$ synthesized can be used for release and oxygen storage or doped with luminescent centers for multimodal medical imaging applications.

References

1. Osseni, S.A., Lechevallier, S., Verelst, M., Dujardin, C., Dexpert, J.G., Neumeyer, D., Leclercq, M., Baaziz, H., Cussac, D., Santran, V., Mauricot, R.: New nanoplatform based on Gd_2O_2S:Eu^{3+} core: synthesis, characterization and use for in vitro bio-labelling. J. Mater. Chem. **21**, 18365 (2011)
2. Osseni, S.A., Lechevallier, S., Verelst, M., Perriat, P., Dexpert, J.G., Neumeyer, D., Garcia, R., Mayer, F., Djanashvili, K., Peters, J.A., Magdeleine, E., Gros-Dagnac, H., Celsis, P., Mauricot, R.: Gadolinium oxysulfide nanoparticles as multimodal imaging agents for T-2-weighted MR, X-ray tomography and photoluminescence. Nanoscale. **6**, 555–564 (2014)
3. Hoenderdaal, S., Espinoza, L.T., Marscheider-Weidemann, F., Graus, W.: Can a dysprosium shortage threaten green energy technologies? Energy. **49**, 344 (2013)
4. Haynes, W.M.: Handbook of chemistry and physics. CRC Press/ Taylor and Francis, Boca Raton (2014)
5. Zhukov, S., Yatsenko, A., Chernyshev, V., Trunov, V., Tserkovnaya, E., Anston, O.: Structural study of lanthanum oxysulfate $(LaO)_2SO_4$. Mater. Res. Bull. **32**, 43–50 (1997)

6. Ye, X., Collins, J.E., Kang, Y., Chen, J., Chen, D.T.N., Yodh, A.G., Murray, C.B.: Morphologically controlled synthesis of colloidal upconversion nanophosphors and their shape-directed self-assembly. Proc. Natl. Acad. Sci. **107**, 22430–22435 (2010)

7. Rodrigues, R.V., Marciniak, L., Khan, L.U., Matos, J.R., Brito, H.F., Stręk, W.: Luminescence investigation of Dy_2O_2S and $Dy_2O_2SO_4$ obtained by thermal decomposition of sulfate hydrate. J Rare Earths. **34**(8), 814 (2016)

8. Andreev, O.V., Denisenko, Y.G., Sal'nikova, E.I., Khritokhin, N.A., Zyryanova, K.S.: Specifics of reactions of cerium sulfate and europium sulfate with hydrogen. Russ. J. Inorg. Chem. **61**(3), 296–301 (2016)

9. Srivastava, A.M., Setlur, A.A., Comanzo, H.A., Gao, Y., Hannah, M.E., Hughes, J.A., Happek, U.: Optical spectroscopy and thermal quenching of the Ce^{3+} luminescence in yttrium oxysulfate, $Y_2O_2[SO_4]$. Opt. Mater. **30**, 1499–1503 (2008)

10. Andreev, P.O., Sal'nikova, E.I., Andreev, O.V., Denisenko, Y.G., Kovenskii, I.M.: Synthesis and upconversion luminescence spectra of $(Y_{1-x-y}Yb_xEr_y)_2O_2S$ solid solutions. Inorg. Mater. **53**(2), 200–206 (2017)

11. Zhang, D.J., Eto, M., Ikeue, K., Machida, M.: Low-temperature synthesis of porous praseodymium oxysulfate oxygen storage materials by using a CTA template. J. Ceram. Soc. Jpn. **115**, 597–601 (2007)

12. Shen, W., Naito, S.: Easy precipitation method for preparation of cerium added $La_2O_2SO_4$ used for oxygen storage. Adv. Mater. Res. **886**, 196–199 (2014)

13. Liu, Y., Tu, D., Zhu, H., Chen, X.: Lanthanide-doped luminescent nanoprobes: controlled synthesis, optical spectroscopy, and bioapplications. Chem. Soc. Rev. **42**, 6924–6958 (2013)

14. Zhang, W., Martinelli, J., Mayer, F., Bonnet, C.S., Szeremeta, F., Djanashvili, K.: Molecular architecture control in synthesis of spherical Ln-containing nanoparticles. RSC Adv. **5**, 69861–69869 (2015)

15. Wang, X., Molokeev, M.S., Zhu, Q., Li, J.G.: Controlled hydrothermal crystallization of anhydrous $Ln_2(OH)_4SO_4$ as a new family of layered rare-earth hydroxide (Ln = Eu-Lu and Y). Chem. Eur. J. (2017). https://doi.org/10.1002/chem.201703282

16. Joliver J.P., Henry M., Livabe J.: De la solution à l'oxyde, Savoirs actuels InterEditions/CNRS (1994)

17. Lian, J., Sun, X., Li, X.: Synthesis, characterization and photoluminescence properties of $(Gd\ 1 − x,\ Eu\ x)_2\ O_2SO_4$ sub-microphosphors by homogeneous precipitation method. Mater. Chem. Phys. **125**, 479–484 (2011)

18. Lian, J., Wang, W., Wang, B.: Photoluminescence of $(Gd_{1-x}, Dy_x)_2O_2SO_4$ phosphors synthesized by homogeneous precipitation method. Adv. Mater. Res. **299**, 612–615 (2011)

19. Lechevallier, S., Lecante, P., Mauricot, R., Dexpert, H., Dexpert-Ghys, J., Kong, H., Kong, H.K., Law, G.L., Wong, K.L.: Gadolinium–europium carbonate particles: controlled precipitation for luminescent biolabeling. Chem. Mater. **22**, 6153–6161 (2010)

20. Andreev, P.O., Sal'nikova, E.I., Kislitsyn, A.A.: Kinetics of the transformation of $Ln_2O_2SO_4$ into Ln_2O_2S (Ln = La, Pr, Nd, and Sm) in a hydrogen flow. Russ. J. Phys. Chem. A **87**, 9 (2013)

21. Andreev, P.O., Sal'nikova, E.I., Kovenski, I.M.: Preparation of LnOS (Ln = Gd, Dy, Y, Er, Lu) in flowing hydrogen and hydrogen sulfide. Inorg. Mater. **50**(10), 1018–1023 (2014)

22. Villars, P.: Material phases data system (MPDS), CH-6354 Vitznau, Switzerland SpringerMaterials (2017). http://materials.springer.com/. Accessed 5 May 2017

23. Liu, G.X., Hong, G.Y., Wang, J.X., Dong, X.T.: Hydrothermal synthesis of spherical and hollow Gd_2O_3: Eu^{3+} phosphors. J. Alloy. Comp. **432**, 200–204 (2007)

Publisher's Note

Springer Nature remains neutral with regard to jurisdictional claims in published maps and institutional affiliations.